Materials Research Express

PAPER

RECEIVED
21 September 2016

REVISED
2 December 2016

ACCEPTED FOR PUBLICATION
13 December 2016

PUBLISHED
24 January 2017

Photo-induced electronic properties in single quantum well system: effect of excitonic lifetime

Jayita Patwari[1], Hemant Ghadi[2], Samim Sardar[1], Jashan Singhal[2], Binita Tongbram[2], Sanjib Shyamal[3], Chinmoy Bhattacharya[3], Subhananda Chakrabarti[2], Samir Kumar Pal[1]

[1] Department of Chemical, Biological and Macromolecular Sciences, S N Bose National Centre for Basic Sciences, Block JD, Sector III, Salt Lake, Kolkata 700106, India
[2] Department of Electrical Engineering, Indian Institute of Technology Bombay, Powai, Mumbai 400076, India
[3] Department of Chemistry, Indian Institute of Engineering Science and Technology Shibpur, P O— Botanic Garden, Howrah 711103, India

E-mail: subho@ee.iitb.ac.in **(S Chakarabarti) and** skpal@bose.res.in **(S K Pal)**

Keywords: excitonic lifetime, carrier holding capacity, photo induced capacitance, GaAs/AlGaAs quantum well

Abstract

In the present study, we have established a correlation between the photo-induced electronic phenomena and excited state lifetime of the photo generated carriers in double barrier $Al_{0.3}Ga_{0.7}As$\GaAs quantum well (QW) structures. The excited state lifetime was measured experimentally by picosecond time resolved photoluminescence spectroscopy for two samples with different well widths (5.3 nm and 16.5 nm). The faster nonradiative decay time of the narrower well can be attributed to the facile escape of electrons from well to barrier due to lower associated energy compared to that of the thicker well which resembles the simulated results of the energy level distribution. The proposed mechanism of carrier escape is further proven from the higher value of unconventional excitonic capacitance value in the thicker well, measured by impedance spectroscopy. The dependence of photo-induced capacitance on well thickness is explained by the lifetime of the excited carriers in this study. Dependence of the photo-generated capacitance (C) on externally applied bias voltage (V) was also studied to quantitatively establish a proportional relation between the carrier holding capacity of the well and the excitonic lifetime. The higher accumulation of charge and lower ground state energy of the thicker well is evident from the higher tunnelling current found for the same in the photocurrent (I) versus voltage (V) measurement. Thus the escape of electrons from the well to barrier is the key factor affecting the photo generated charge accumulation and its holding capacity which in turn influences the device performances.

1. Introduction

Before the 1970s the achievable band gaps in the field of semiconductor optoelectronics were fully dependent on the properties of common III–V materials like GaAs and its alloy materials e.g. AlGaAs, InGaAs etc. Discovery of quantum well (QW) and super lattice structures in the year of 1970 by *Esaki* and *Tsu* [1] lead to immense growth in this field. Since then a mammoth number of studies have been done to explore the basic physical properties of quantum confinement and their use in fabrication of optoelectronic devices such as light emitting diodes (LED) [2], diode lasers [3], quantum cascade lasers [4], solar cells [5], avalanche photodiode [6], inter-sub-band detectors [7], unipolar avalanche photodiode [8], modulators [9], and photo detectors [10]. In QW samples, confinement energy (well width) offers an extra degree of freedom which helps to tune the emission wavelength. The fascinating features of QW structures are due to the quasi-2D carrier system which arises mainly due to the localization of excitons. There are lots of particle exchange processes involved in QW samples such as conversion of free electrons and holes from bound excitons, defect state trapping, recreation of photons due to the annihilation of electrons and holes etc [11]. Depending on the barrier height [12] and well width, the physical properties of QWs change widely due to the change in extent of confinement. The variations of physical properties depending on the change of well thickness were reported earlier but the approach to resolve physical processes is often oversimplified [13]. Despite the large number of reports on QW structures and about their physical properties, there are still

uncertainties about various thermal escape [14], tunnelling [15], inter-subband relaxation [16] and other non-radiative processes [17] and their relative importance specially in device application at room temperature.

In this study, we have mainly focused on the explanations of the large photo-induced capacitance observed in GaAs/AlGaAs single QW and the correlation of this phenomena with the excited state lifetime of the carriers. In recent literature this type of light induced unconventional capacitance generation is discussed in the case of two dimensional electron systems (2DES) such as oxide-semiconductor interfaces [18], and QWs in III–V material heterojunctions [19]. The phenomena of light induced capacitance in 2DES has been used in fabricating capacitance based photo detectors [20–22]. The same structures can be used for resonant tunnel diodes [23] and charge coupled devices [24]. It was also reported recently that the density modulation of the light generated carriers can enhance the capacitance value [25] and the quantum mechanical description of the enhanced capacitance was given in terms of correlation and exchange energies in recent literature [22]. We have given experimental evidence to the explanations of enhanced light induced capacitance using spectroscopic tools and established a correlation between the optical and electronic properties. A lot of optical studies have been done on these systems in the literature but the excitonic behaviours i.e. lifetime and carrier holding capacities have never been correlated with photo-induced electrical phenomena. The picosecond time resolved photoluminescence (TRPL) studies for the QW samples have been done to get a convincing explanation of the carrier escape mechanism from the well and its dependence on the well thickness. Comparison between the photo-induced inbuilt capacitance and resistance of these undoped QW samples by electrochemical impedance spectroscopy (EIS) implies that the charge accumulation capability of the insulating media is very much dependent on well thickness. By analysing this light induced capacitance we have given a proof of the well to barrier escape process to be the main nonradiative path of losing carriers. From the capacitance (C)–voltage (V) measurement it was proven that the higher value of capacitance in the thicker well was due to the higher charge holding capacity. The quantitative estimation of photocurrent generated from different samples with different width is convincingly correlated with the energy level distribution and escape mechanism of the electrons. Thus, in this present study we have successfully explained the two components of excitonic lifetime by correlating them with the light induced electronic phenomena which are solely dependent on the exciton generation, the carrier holding capacity of the confined structure and the loss mechanisms.

2. Experimental section

2.1. Preparation of sample

The GaAs/$Al_{0.27}Ga_{0.73}As$ single QW structures, used in this study, as shown in figure 1(a), were grown using an Riber Sys 14020 Epineat a solid-source molecular beam epitaxy (MBE) furnished with Ga and Al effusion cells and As cracker. The sample was grown on a semi insulating GaAs (0 0 1) substrate layer at a growth temperature of 590 °C. Quantum structure were overgrown on 200 nm GaAs buffer layer. The GaAs well layer of thickness (L_z) was sandwiched between 25 nm thick $Al_{0.27}Ga_{0.73}As$ barrier layers and then capped with a 3 nm thick intrinsic GaAs layer on the top. The only structural difference between the two samples was the well width. For one sample it was 5.3 nm and for the other it was 16.5 nm. The structures shown in figure 1(a) were used for the spectroscopic characterization techniques but for studies regarding electronic properties, vapour deposition of Indium was done on both sides of the sample to make the metallic contacts as shown in figure 4(a). The deposition chamber pressure was maintained at 5×10^{-6} mbar throughout the process. On the growth side a 250 nm layer of Indium was made while on the bottom side of the sample the Indium layer thickness was 200 nm. An optical aperture was inserted on the growth side by using a circular shadow mask during deposition.

2.2. Characterization methods

Cross-sectional transmission electron microscopy (XTEM) was used to explore the morphology of the QW samples and to get an idea about the exact GaAs well thicknesses. The samples were prepared using a standard TEM sample preparation technique. XTEM images were carried out on JEOL JEM 2010F electron microscope system operating at 200 kV. To maintain the temperature during photoluminescence (PL) the whole study was done keeping the sample pieces in a closed cycle helium cryostat. A continuous wave solid state laser of 532 nm wavelength was used as an excitation source. The steady state PL both at 19 K and at room temperature was measured at 25 mW power of the excitation source. For dispersion and detection of the luminescence a liquid nitrogen-cooled InGaAs array detector was used. A time correlated single photon counting (TCSPC) setup was used to study TRPL.The instrument response function (IRF) was 70 ps. For this study we used a pulsed laser source of 409 nm wavelength for excitation. The experimental set up and methodology in this regard were described in detail in our earlier publications [26, 27].

A MATLAB based QW simulation was carried out to calculate the first three energy level transitions which correspond to the transitions between ground, first and second excited states of conduction band and valence band in QW. In the simulation, we have used the finite difference method for calculating the Hamiltonian matrix while taking into account the effective mass differences at the interfaces. We have discretized the position variable

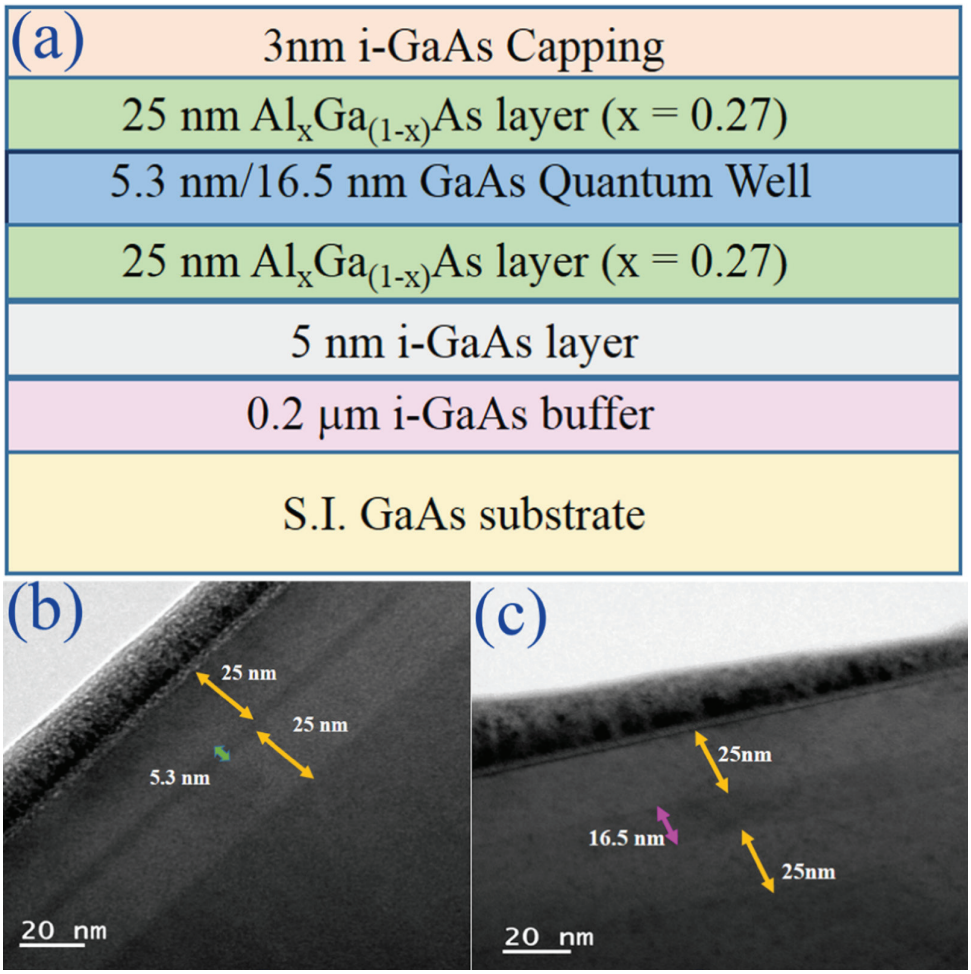

Figure 1. (a) Structure of QW samples with well width 5.3 nm and 16.5 nm, (b) TEM image of sample with 5.3 nm well width, (c) TEM image of sample with 16.5 nm well with.

x into a lattice of points such that the spacing between two points is equal to **a** which is the smallest unit of the cube mesh. The theoretical calculation becomes exact only in the limit **a** tending to 0 i.e. smaller the mesh more accurate is the result. For simulation purpose, we have chosen $N_b = 25$ nm (AlGaAs width) and variable GaAs width (N_w) though both of the parameters can be varied in the simulation. The value of ΔE_c was considered to be 0.2469 eV at 19 K and 0.2468 eV at 300k. Also we have used infinite wall boundary conditions where the potential is infinitely large at the beginning and ending at a discrete point (the specific value of potential at the end point will not matter as long as the wave function is zero).

The EIS and capacitance–voltage (CV) experiments were carried out on an electrochemical workstation CHI650E (CH instruments). The impedance measurement was performed under varying frequency range from 0.1 Hz to 5 kHz under open circuit condition. The frequency was kept at 1000 Hz during the CV measurements. The active areas of the samples were illuminated under 100 mW cm^{-2} condition, using 300 W Xe lamp source (Excillitus, USA), during the impedance measurements. The fitting of the spectra was done using the CHI650E software in order to get the appropriate equivalent circuit. The current density (I)–voltage (V) characteristics of the QW samples were recorded by a Keithley multimeter with a constant irradiation source of 100 mW cm^{-2}.

3. Results and discussion

3.1. Material characterization

The only difference between the two samples of this study is the well thickness which is confirmed by the TEM images shown in figures 1(b) and (c). It is clearly depicted in the TEM images that the well thicknesses are 5.3 nm and 16.5 nm, respectively while the barrier thicknesses are 25 nm in both the cases. Another notable feature which can be mentioned from figures 1(b) and (c) is that the flat interfaces and good homogeneity. The barrier layer

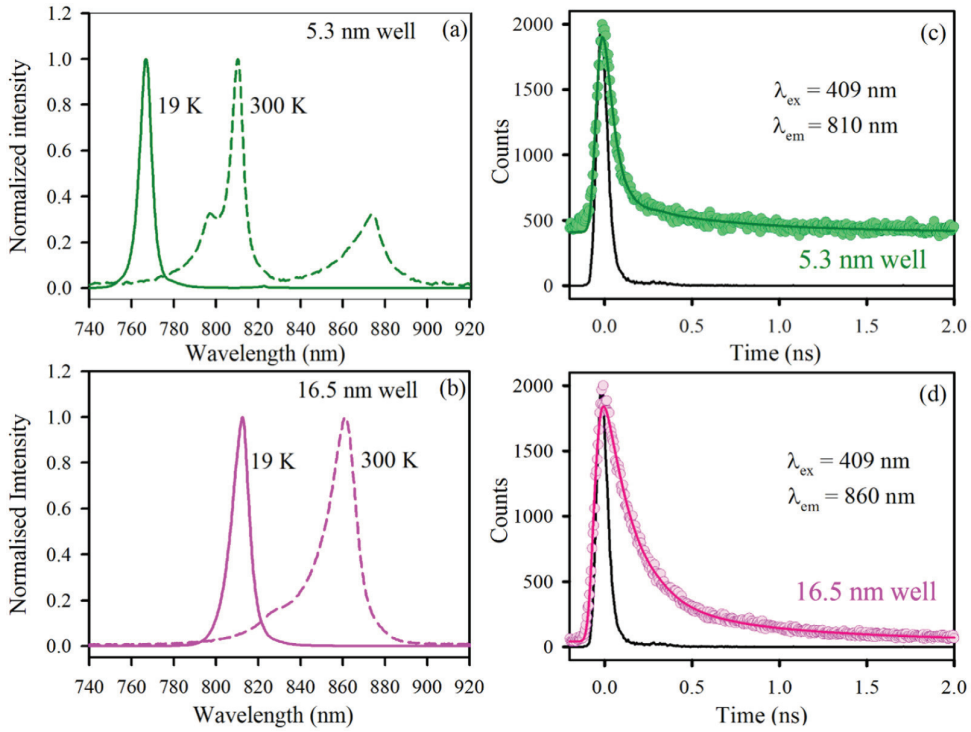

Figure 2. (a) and (b) Steady state photoluminescence spectra of 5.3 nm well and 16.5 nm well, respectively, (c) and (d) time resolved photoluminescence spectra of 5.3 nm well and 16.5 nm well, respectively.

($Al_xGa_{(1-x)}As$) bandgap of 1.74 eV was calculated using Vegard's law. The steady state PL spectra measured at 19 K and 300 K temperatures are represented in figures 2(a) and (b) for the thin and thick well sample, respectively. It is evident that the QW samples have only one prominent emission at lower temperature i.e. from first electronic ($n = 1$) level to first heavy hole (HH1) level. The peak position of the 16.5 nm well is at ~45 nm higher wavelength than the ~5.3 nm well. This is because of the difference in confinement energy as explained by simulated results as described below. The peak positions are red shifted at 300 K temperature than that of 19 K temperature because of the decrease in band gap with increase in temperature according to Varshini's Law [28]. Notable difference between the spectra of 19 K and 300 K is the presence of a shoulder at the higher energy side of the peak for the second case. This peak accounts for the transition from $n = 1$ electronic state to the light hole state of the confined structure [29–32]. This transition becomes visible only at higher temperatures because at temperatures below 100 K the light hole valence band level was not thermally populated and thermal equilibrium between the electrons and the light hole is a necessary condition for the transition to take place [33]. For the 5.3 nm well sample, the lower intensity peak at 870 nm is probably due to the GaAs substrate layer. In the case of the 16.5 nm well that substrate layer peak is masked by the peak from $n = 1$ to heavy hole level transition. Activation energies (E_{a1}) from the first electronic state of the QW were calculated from the temperature dependent PL for both the samples. Using Gaussian fitting, the area under the curve was calculated and used in a double variable exponential decay function. Activation energy for first electronic state was calculated at higher temperature where the equation became 1D and from the slope of linear fitting at high temperatures (equation (1)). The reduced equation is given as,

$$I(T) = \frac{I(0)}{1 + A\exp\left(-\frac{E_{a1}}{kT}\right)} \quad (1)$$

where $I(T)$ and $I(0)$ are the area under the curve fitted from Gaussian fitting at 19 K and 300 K, respectively. A is constant, k is the Boltzmann constant and E_{a1} is the activation energy for first electronic state. The magnitude of E_{a1} for the thinner well was found to be ~87.26 meV and that for the thicker one is ~191.6 meV.

Figures 2(c) and (d) represent the picosecond resolved PL decay of the two samples. From the excited state carrier lifetimes mentioned in table 1, it can be noted that both the QW samples have a faster time component due to the presence of non-radiative pathways. It is well documented in the literature that charge carriers in sufficiently narrow QWs have more than an order of magnitude shorter lifetime than those observed in bulk material of comparable quality [13, 34, 35]. The faster nonradiative process occurring is due to a localization-induced reduction of radius in 2D exciton [13, 29, 34, 36]. At room temperature, recombination occurs between free carriers not between excitons

Table 1. Fitted decay time constant of QW samples from picosecond resolved PL experiments[a].

Sample	τ_1 (ps)	τ_2 (ps)	τ_{avg} (ps)
5.3 nm well	45 (93%)	650 (7%)	87.35
16.5 nm well	150 (87%)	846 (13%)	240.48

[a] Numbers in the parenthesis indicate relative weightages.

[37]. The characteristic time of exciton formation from free carriers lies in the range from several tens to hundreds of picoseconds [38–42]. The exciton thermalization in the reservoir occurs approximately in the same time range [38, 43–45]. Width dependent study of the recombination dynamics were also done previously by various groups [13, 46] and the recombination time has been seen to decrease monotonically with the decreasing well thickness. In our study, the initial faster component of carrier life time was observed to be 45 ps for the thinner well and 150 ps in the case of the thicker well. The relative percentage of the faster time component is nearly the same for both. The same non radiative mechanistic pathway is attributed to explain the faster component in both the cases. As a non-resonant excitation source has been used, nonradiative recombination in GaAs channels as well as in AlGaAs barrier is equally probable [47]. We propose the thermal escape of the free carriers from the well towards the barrier is the predominant factor to monitor the faster time scale of PL decay which can also be correlated with the activation energy values. The energy difference between the well and the barrier is smaller in the case of the thinner well than that of the thicker as described by the energy level distribution earlier. As a consequence the τ_1 is much slower in the case of the thicker well. PL and TRPL results are in coherence with each other and as expected high activation energy is required for the carriers to escape from the thicker well. Slower carrier lifetime indicates formation of loosely bound exciton in the thicker well which can be applicable in charge migration based devices. Device characterization was carried out in presence of light to explore this charge migration possibility in current QW structures.

3.2. Simulation results

The energy level values calculated using MATLAB simulation for four different well widths are shown in figure 3(b). The model used for the calculation is shown in figure 3(a) and the respective notations, terms and parameters are mentioned in tables 2 and 3. The energy levels calculated from the code are in good agreement with PL peak energies, as evident from figure 3(c). As explained from the experimental results the difference between ground state and excited state energies is higher in the thinner well which is evident from our simulation results. With increase in well thickness a reduction in energy spacing was observed which reduces resonant tunnelling effect. This higher spacing between the ground state and excited state energies in thinner well results in negative resistance which is further proved from current–voltage characteristics in the device characterization section.

3.3. Device characterization

A significant increase in capacitance for both the QW samples was observed upon light irradiation. The behaviour of the whole system can be considered as a metal–insulator–metal capacitor. Generation of light induced capacitance is due to charge separation forming exciton in presence of photons and the system behaves as a parallel plate capacitor with two different junctions. Semi insulating GaAs substrate to metal junction capacitance can be neglected as it is too thick and the carrier concentration is significantly low. To quantitatively measure the photo induced capacitance for QW samples, the analysis of impedance spectra was carried out as shown in figure 4(b) and fitted the data with an equivalent RC circuit which has one inbuilt geometric resistance (ohmic) and two resistance–capacitance circuits as shown in the inset of figure 4(b). The associated parameters are summarized in table 4. The high frequency limit in the Nyquist plot accounts for the geometric resistance in our study and that value is of the same order of magnitude for both the QW samples. It is clear from figure 4(b) that for both the samples there are two semi circles in which the higher frequency one is the characteristic of the interface of metal and capping GaAs layer. Resistance and capacitance values representing the semicircle at the higher frequency side do not show significant variation. The associated resistance with the semicircle at the lower frequency side differs by order of magnitude with the increase in the well thickness. This semicircle represents the junction of the well with the capping GaAs layer. As shown in table 4, the capacitance (C_2) increases with increase in well width and correspondingly the resistance (R_2) value decreases. The explanation behind the larger capacitance value is the better charge accumulation in the case of the wider well, as proved earlier from the excited state lifetime measurements. Resistance (R_2) is greater in the case of the narrower well because decreasing well thickness results in increase in distribution of trapping states [48]. Capacitance–resistance characteristics obtained through impedance spectroscopy can be useful in the field of capacitance-based photo detectors [20].

To quantitatively measure the carrier concentration associated with the increased capacitance upon light irradiation the capacitance–voltage (CV) characterization were performed. Figures 4(c) and (d) represent Mott–Schottkey plots for the thicker and thinner well, respectively. The method used in this study for the quantitative estimation of carrier concentration in QW sample was originally developed by Kreher in 1993 [49].

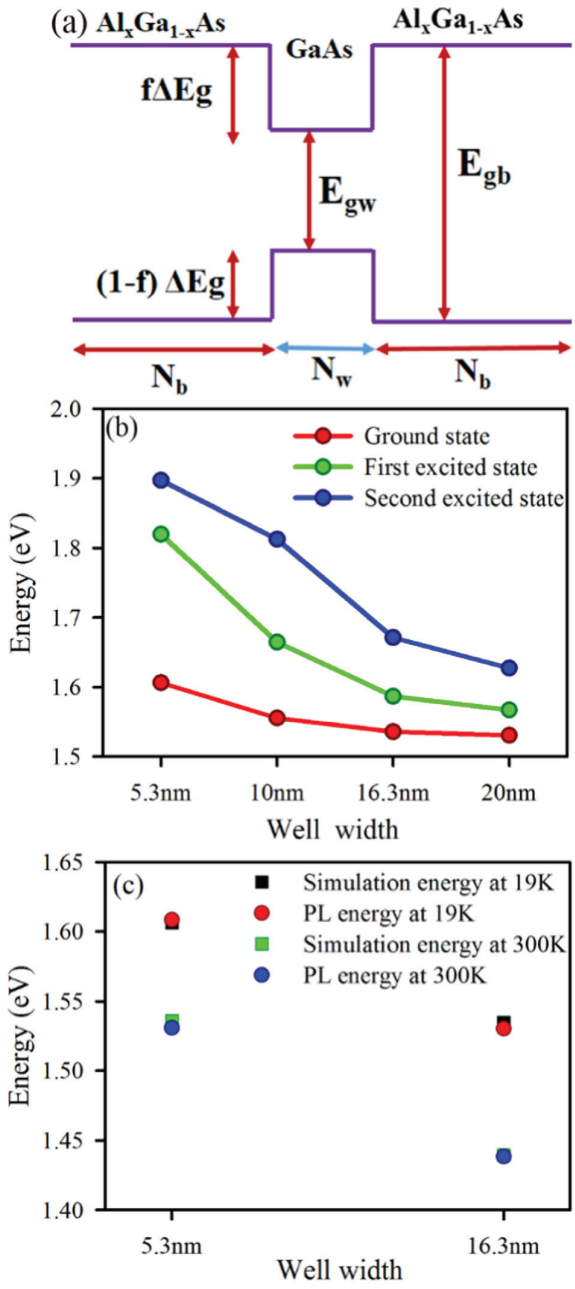

Figure 3. (a) Model used for simulation (terms and notations are described in tables 2 and 3), (b) graphical representation of calculated energy values for different well widths. (c) Comparison of experimental and calculated energy values.

The carrier concentration at different junctions were measured by fitting the Mott–Schottkey data with the following equation,

$$\frac{1}{C^2} = \frac{2V}{\varepsilon\varepsilon_0 N_1 e} + \left(1 - \frac{N_w}{N_1}\right)\frac{(2d_2 + d)d}{(\varepsilon\varepsilon_0)^2} + \left(1 - \frac{N_2}{N_1}\right)\frac{d_2^2}{(\varepsilon\varepsilon_0)^2} \quad (2)$$

where C is the total capacitance, V is the applied bias, ε and ε_0 are the permittivity of well and free space. Permittivity constants for GaAs and AlGaAs are $12.9\varepsilon_0$ and $12.19\varepsilon_0$, respectively. Permittivity constant of the well was considered as an effective permittivity constant calculated from GaAs and AlGaAs. N_w is the total carrier concentration in the well, N_1 and N_2 are the carrier concentrations in the capping layer and semi-insulating substrate GaAs layer respectively, d_2 is the capping layer thickness and d is the thickness of the AlGaAs/GaAs/AlGaAs heterojunction. The capping layer is assumed to be of i-GaAs layer (3 nm) and the total well thicknesses are 55.3 nm and 66.5 nm. The carrier concentration of the semi-insulating wafer (N_2) is much lower than capping layer (N_1) so the later part of the expression i.e. ratio of N_2/N_1 can be ignored. The simplified expression used in the calculation is given below,

Table 2. Notations and terms used in simulation.

E_{gw}	Band gap of the well
E_{gb}	Band gap of the barrier
f	GaAs–AlGaAs band gap discontinuity percentage for electrons
N_b	Barrier width in terms of number of discrete points
N_w	Well width in terms of number of discrete points
x	Alluminum percentage in AlGaAs
m	Mass of electron in free space
m_{we}	Effective mass of electron in well
m_{be}	Effective mass of electron in barrier
m_{wh}	Effective mass of hole in the well
m_{bh}	Effective mass of hole in the barrier
T	Measurement temperature

Table 3. Material parameters as obtained from NSM archive.

E_{gw}	$1.519–5.405 \times 10^{-4}\, T^2/(T + 204)$
E_{gb}	$1.519 + 1.55x + 0.37x^2 - 5.41 \times 10^{-4}\, T^2/(T + 204)$
f	0.65
m_{we}	0.063 m
m_{be}	$(0.063 + 0.083x)$ m
m_{wh}	0.51 m
m_{bh}	$(0.51 + 0.25x)$ m

$$\frac{1}{C^2} = \frac{2V}{\varepsilon\varepsilon_0 N_l e} + \left(1 - \frac{N_w}{N_l}\right)\frac{(2d_2 + d)d}{(\varepsilon\varepsilon_0)^2} + \frac{d_2^2}{(\varepsilon\varepsilon_0)^2}. \tag{3}$$

The associated carrier concentrations obtained for the thicker well was 2 orders higher than the thinner well which is consistent with the capacitance values obtained from the impedance spectroscopy and the trend in carrier escape phenomena observed in the time resolved PL measurements. The carrier concentration values for different junctions of different samples extracted from the Mott–Schottky measurements are summarized in table 5. In the thicker well these loosely bound excitons can be migrated from one terminal to another which has potential applications in the field of charge coupled devices and photo induced capacitive circuits. Current–voltage characteristics will give further insights in photo generated charge transfer within QW structures which can be related to C–V results.

The current–voltage (I–V) characteristics of both QW samples is shown in figure 4(e). A noteworthy result was increase in output current with increasing well thickness. It can be concluded from the I–V data that the current coming out of the well is due to tunnelling so the whole device performs as a resonant tunnel diode. As the $n = 1$ electronic state is lower in case of the thicker well as shown in figure 1(d), the ground electronic state becomes resonant with the emitter level for much lower bias than the thinner one. So, the thicker well is a better candidate for devices like resonant tunnel diode. For the thinner well sample an anomalous behaviour is observed in the I–V curve nature at ~6 V applied voltage which is illustrated in the inset of figure 4(e). A negative differential resistance is observed in that region of applied bias as the tunnelling current is dropping due the energy mismatch of the ground electronic levels and emitter level and the second electronic level energy reduces due to band bending, then the thermionic emission becomes predominant. The reason behind the higher current associated with the thicker well is that the energy levels are such that thermionic emission current contribution is negligible compared to tunnelling component at higher applied bias. The anomalous behaviour of having higher capacitance and higher current was observed in thicker well sample. It can be explained as the total capacitance in QW structures is a combination of diffusion and junction capacitances. Junction capacitance is inversely related to depletion width which can be assumed to be similar in both QW structures whereas the diffusion capacitance (C_d) is directly proportional to diffusion current (I_d) which is evident from the following equation [50],

$$C_d = \frac{\tau I_d}{\eta V} \tag{4}$$

where τ is the average lifetime of the carrier which is also lower in case of thinner well and η is the generation-recombination co-efficient which is same for both the sample as the same excitation source is used for both the samples in all the studies. The higher tunnelling current for the thicker well is due to higher carrier diffusion

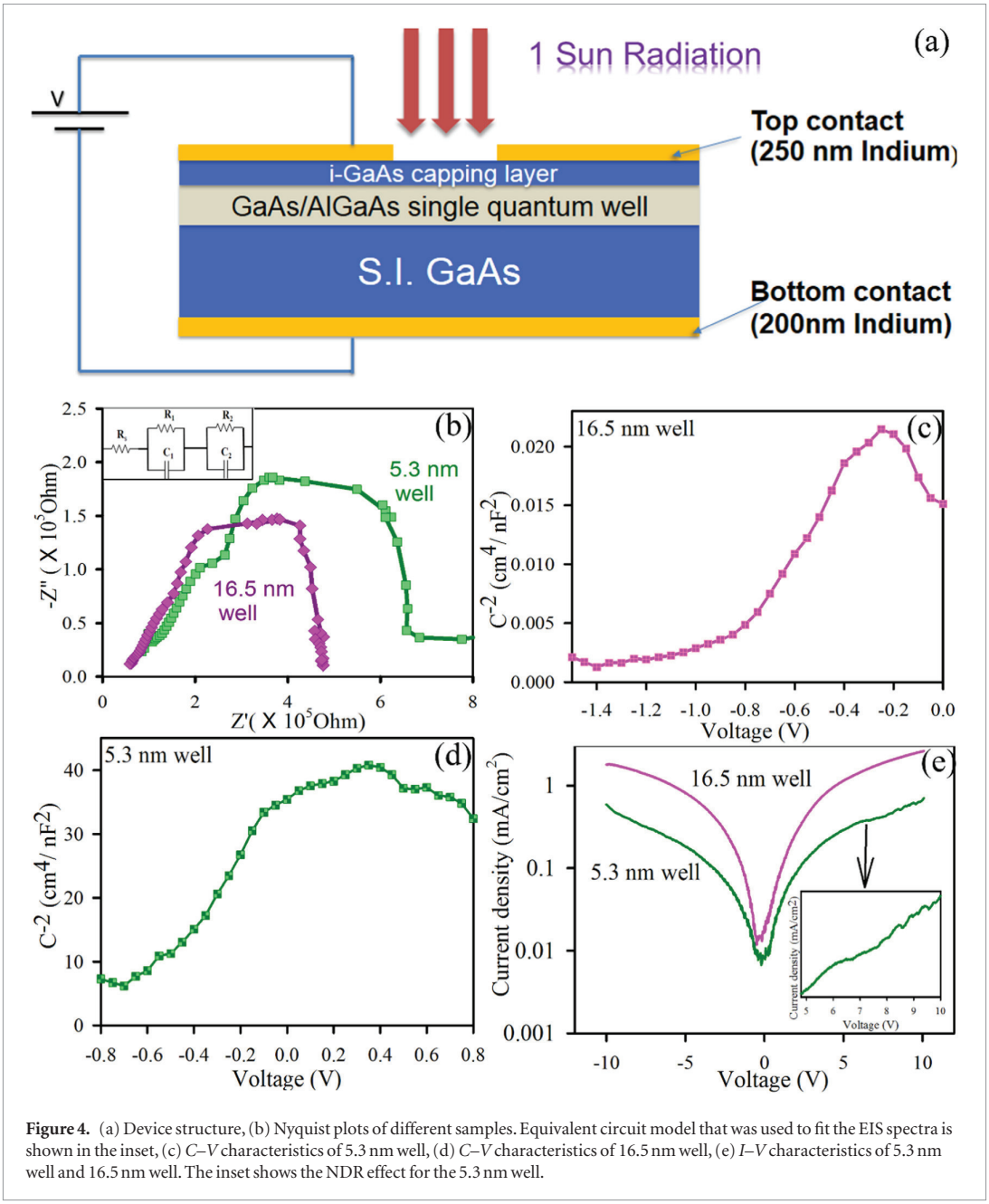

Figure 4. (a) Device structure, (b) Nyquist plots of different samples. Equivalent circuit model that was used to fit the EIS spectra is shown in the inset, (c) *C–V* characteristics of 5.3 nm well, (d) *C–V* characteristics of 16.5 nm well, (e) *I–V* characteristics of 5.3 nm well and 16.5 nm well. The inset shows the NDR effect for the 5.3 nm well.

Table 4. Resistance and capacitance values of different samples estimated from simulated fitting of EIS spectra.

Sample	R_s (Ω)	R_1 (Ω)	R_2 (Ω)	C_1 (F)	C_2 (F)
5.3 nm well	9.27×10^4	5.7×10^5	1.09×10^5	3.34×10^{-8}	3.36×10^{-9}
16.5 nm well	6.45×10^4	3.4×10^5	5.6×10^4	4.5×10^{-8}	8.7×10^{-9}

Table 5. Carrier concentrations at different junction from *C–V* measurements.

Sample	N_1 (cm^{-2})	N_w (cm^{-2})
5.3 nm well	3.07×10^{11}	4.49×10^{11}
16.5 nm well	4.44×10^{13}	4.096×10^{13}

which is consistent with the higher C_d achieved in the same sample. The average carrier lifetime for the thicker well was comparatively higher than the thinner one which will result in more capacitive or charge accumulation with light irradiation and major component was contributed by diffusion capacitance. As diffusion capacitance

is dependent on diffusing current, this capacitance can be used to modulate charge accumulation from one terminal of QW to another.

4. Conclusion

Dependence of the main nonradiative process on well thickness for GaAs/AlGaAs QW samples is revealed by steady state and picosecond resolved PL studies. Temperature dependent PL results exhibit an increase in activation energy with increasing well width. Time resolved PL studies show that the narrower well exhibits a faster decay lifetime compared to that of wider well due to the lower energy barrier which facilitates the thermal escape of the photo generated carriers from the well to barrier. EIS spectroscopy inflicted higher charge accumulation in the thicker well which was modelled with a 2 capacitive *R–C* circuit. The higher charge accumulation is further confirmed from the Mott–Schottky data which was found to be two orders of magnitude higher in the case of the thicker well. The higher photocurrent in the thicker well measured from *I–V* characteristics implies that the source of the current in the case of the thicker one is tunnelling not the thermionic emission. So the predominant nonradiative process is the thermal escape of carriers and that was proven both from electrical and optical signature of the systems. These huge photo generated carriers could be used in future applications of the QW samples in capacitance based photo induced devices and photo generated charge migration based devices like charge coupled devices and resonant tunnel diodes.

Acknowledgment

JP would like to thank CSIR (India) for fellowship. We thank DST (India) for financial grants DST-TM-SERI-FR-117 and SB-S1-PC-011-2013. We also thank DAE (India) for financial grant, 2013-37P-73-BRNS.

References

[1] Esaki L and Tsu R 1970 Superlattice and negative differential conductivity in semiconductors *IBM J. Res. Dev.* **14** 61–5
[2] Krames M *et al* 2002 High-power III-nitride emitters for solid-state lighting *Phys Status Solidi* a **192** 237–45
[3] O'Reilly E P and Adams A R 1994 Band-structure engineering in strained semiconductor lasers *IEEE J. Quantum Electron.* **30** 366–79
[4] Faist J, Capasso F, Sivco D L, Sirtori C, Hutchinson A L and Cho A Y 1994 Quantum cascade laser *Science* **264** 553–6
[5] Barnham K *et al* 1997 Quantum well solar cells *Appl. Surf. Sci.* **113** 722–33
[6] Asamira S, Atsushi Y, Tatsuo Y, Ken I and Yoshimasa O 2002 Dark current reduction of avalanche photodiode using optimized InGaAsP/InAlAs superlattice structure *Japan. J. Appl. Phys.* **41** 1182
[7] Sarath D G, Gabby S, Jin S P, True-Lon L and Barry F L 1994 Infrared detectors reach new lengths *Phys. World* **7** 35
[8] Levine B, Choi K, Bethea C, Walker J and Malik R 1987 Quantum well avalanche multiplication initiated by 10 μm intersubband absorption and photoexcited tunneling *Appl. Phys. Lett.* **51** 934–6
[9] Weiner J S, Miller D A and Chemla D S 1987 Quadratic electro-optic effect due to the quantum-confined Stark effect in quantum wells *Appl. Phys. Lett.* **50** 842–4
[10] Horstmann M *et al* 1995 InP/InGaAs photodetector based on a high electron mobility transistor layer structure: its response at 1.3 μm wavelength *Appl. Phys. Lett.* **67** 106–8
[11] Block D, Romestain R, Edel P and Fränke S 1992 Exciton and free carrier dynamics in GaAs quantum wells: excitation density effects *J. Lumin.* **53** 339–44
[12] Lin G-B *et al* 2013 Effect of quantum barrier thickness in the multiple-quantum-well active region of GaInN/GaN light-emitting diodes *IEEE Photonics J.* **5** 1600207
[13] Göbel E, Jung H, Kuhl J and Ploog K 1983 Recombination enhancement due to carrier localization in quantum well structures *Phys. Rev. Lett.* **51** 1588
[14] Gurioli M, Martinez-Pastor J, Colocci M, Deparis C, Chastaingt B and Massies J 1992 Thermal escape of carriers out of GaAs/$Al_xGa_{1-x}As$ quantum-well structures *Phys. Rev.* B **46** 6922
[15] Leo K *et al* 1990 Effect of collisions and relaxation on coherent resonant tunneling: Hole tunneling in GaAs/$Al_xGa_{1-x}As$ double-quantum-well structures *Phys. Rev.* B **42** 7065
[16] Seilmeier A, Hübner H-J, Abstreiter G, Weimann G and Schlapp W 1987 Intersubband relaxation in GaAs-$Al_xGa_{1-x}As$ quantum well structures observed directly by an infrared bleaching technique *Phys. Rev. Lett.* **59** 1345
[17] Polland H-J *et al* 1988 Hot carrier trapping in GaAs/AlGaAs single quantum wells with different confinement structures *Solid-State Electron.* **31** 341–4
[18] Li L, Richter C, Paetel S, Kopp T, Mannhart J and Ashoori R 2011 Very large capacitance enhancement in a two-dimensional electron system *Science* **332** 825–8
[19] Zhao X *et al* 2006 Optically modulated high-sensitivity heterostructure varactor *IEEE Electron Device Lett.* **27** 710–2
[20] Dianat P, Prusak R W, Persano A, Quaranta F, Cola A and Nabet B (ed) 2012 Giant light-induced capacitance enhancements in an unconventional capacitor with two-dimensional hole gas *Photonics Conf. (IPC)* (Burlingame, CA: IEEE) (doi: 10.1109/IPCon.2012.6358861)
[21] Horstmann M *et al* 1995 InP/InGaAs photodetector based on a high electron mobility transistor layer structure: its response at 1.3 μm wavelength *Appl. Phys. Lett.* **67** 106–8
[22] Dianat P, Persano A, Quaranta F, Cola A and Nabet B 2015 Anomalous capacitance enhancement triggered by light *IEEE J. Sel. Top. Quantum Electron.* **21** 228–32
[23] Sharma V and Singh R P 2013 Nano scale simulation of GaAs based resonant tunneling diode *Int. J. Eng. Comput. Sci.* **2** 3580–3
[24] Goodhue W 1989 Using molecular-beam epitaxy to fabricate quantum-well devices *Linc. Lab. J.* **2** 183–205
[25] Dianat P *et al* 2012 A highly tunable heterostructure metal-semiconductor-metal capacitor utilizing embedded 2 dimensional charge *Appl. Phys. Lett.* **100** 153505

[26] Sardar S, Kar P and Pal S K 2014 The impact of central metal ions in Porphyrin functionalized ZnO/TiO_2 for enhanced solar energy conversion *J. Mater. Nanosci.* **1** 12–30
[27] Sardar S, Sarkar S, Myint M T Z, Al-Harthi S, Dutta J and Pal S K 2013 Role of central metal ions in hematoporphyrin-functionalized titania in solar energy conversion dynamics *Phys. Chem. Chem. Phys.* **15** 18562–70
[28] Varshni Y P 1967 Temperature dependence of the energy gap in semiconductors *Physica* **34** 149–54
[29] Christen J and Bimberg D 1986 Recombination dynamics of carriers in GaAs-GaAlAs quantum well structures *Surf. Sci.* **174** 261–71
[30] Fouquet J and Siegman A 1985 Room-temperature photoluminescence times in a GaAs/Al_xGa_{1-x}As molecular beam epitaxy multiple quantum well structure *Appl. Phys. Lett.* **46** 280–2
[31] Fouquet J, Siegman A, Burnham R and Paoli T 1985 Carrier trapping in room-temperature, time-resolved photoluminescence of a GaAs/Al_xGa_{1-x}As multiple quantum well structure grown by metalorganic chemical vapor deposition *Appl. Phys. Lett.* **46** 374–6
[32] Miller R, Kleinman D, Tsang W and Gossard A 1981 Observation of the excited level of excitons in GaAs quantum wells *Phys. Rev.* B **24** 1134
[33] Polland H-J, Rühle W, Kuhl J, Ploog K, Fujiwara K and Nakayama T 1987 Nonequilibrium cooling of thermalized electrons and holes in GaAs/Al_xGa_{1-x}As quantum wells *Phys. Rev.* B **35** 8273
[34] Christen J, Bimberg D, Steckenborn A and Weimann G 1984 Localization induced electron–hole transition rate enhancement in GaAs quantum wells *Appl. Phys. Lett.* **44** 84–6
[35] Bimberg D, Christen J, Steckenborn A, Weimann G and Schlapp W 1985 Injection, intersubband relaxation and recombination in GaAs multiple quantum wells *J. Lumin.* **30** 562–79
[36] Bastard G, Mendez E, Chang L and Esaki L 1982 Exciton binding energy in quantum wells *Phys. Rev.* B **26** 1974
[37] Fouquet J E and Burnham R D 1986 Recombination dynamics in GaAs/Al_xGa_{1-x}As quantum well structures *IEEE J. Quantum Electron.* **22** 1799–810
[38] Trifonov A *et al* 2015 Nontrivial relaxation dynamics of excitons in high-quality InGaAs/GaAs quantum wells *Phys. Rev.* B **91** 115307
[39] Piermarocchi C, Savona V, Quattropani A, Schwendimann P and Tassone F 1997 Photoluminescence and carrier dynamics in GaAs quantum wells *Phys. Status Solidi* a **164** 221–5
[40] Bajoni D, Senellart P, Perrin M, Lemaitre A, Sermage B and Bloch J 2006 Exciton dynamics in the presence of an electron gas in GaAs quantum wells *Phys Status Solidi* b **243** 2384–8
[41] Szczytko J, Kappei L, Berney J, Morier-Genoud F, Portella-Oberli M and Deveaud B 2004 Determination of the exciton formation in quantum wells from time-resolved interband luminescence *Phys. Rev. Lett.* **93** 137401
[42] Portella-Oberli M, Berney J, Kappei L, Morier-Genoud F, Szczytko J and Deveaud-Plédran B 2009 Dynamics of trion formation in In_xGa_{1-x}As quantum wells *Phys. Rev. Lett.* **102** 096402
[43] Basu P and Ray P 1992 Energy relaxation of hot two-dimensional excitons in a GaAs quantum well by exciton-phonon interaction *Phys. Rev.* B **45** 1907
[44] Piermarocchi C, Tassone F, Savona V, Quattropani A and Schwendimann P 1996 Nonequilibrium dynamics of free quantum-well excitons in time-resolved photoluminescence *Phys. Rev.* B **53** 15834
[45] Ivanov A, Littlewood P and Haug H 1999 Bose–Einstein statistics in thermalization and photoluminescence of quantum-well excitons *Phys. Rev.* B **59** 5032
[46] Hariz A, Dapkus P D, Lee H, Menu E and DenBaars S 1989 Minority-carrier lifetimes in undoped AlGaAs/GaAs multiple quantum wells *Appl. Phys. Lett.* **54** 635–7
[47] Fang Y *et al* 2015 Investigation of temperature-dependent photoluminescence in multi-quantum wells *Sci. Rep.* **5** 1–7
[48] Bisquert J 2008 Beyond the quasistatic approximation: Impedance and capacitance of an exponential distribution of traps *Phys. Rev.* B **77** 235203
[49] Kreher K 1993 Capacitance–voltage characteristics of a quantum well within a Schottky layer *Phys Status Solidi* a **135** 597–603
[50] Bakshi U and Godse A 2009 *Analog Electronics* (Pune: Technical Publications)